DOI: 10.1002/ejoc.200900689

DFT Study on Tautomerism of Dihydro-2*H*-1,5-benzodiazepin-2-ones and Dihydro-2*H*-1,5-benzodiazepine-2-thiones

Sergiy I. Okovytyy,*[a,b] Liudmyla K. Sviatenko,[b,c] Alexandr A. Gaponov,[a] Liliya I. Kasyan,[a] Igor N. Tarabara,[a] and Jerzy Leszczynski[b]

Keywords: Nitrogen heterocycles / Tautomerism / Density functional calculations

DFT calculations were performed to study the tautomeric rearrangements in the isolated, monoethanol- and diethanol-solvated, and dimeric forms of 4-methyl-1,3-dihydro-2*H*-1,5-benzodiazepin-2-one and 4-methyl-1,3-dihydro-2*H*-1,5-benzodiazepine-2-thione. Molecular geometries of the tautomers and transition state structures were optimized at the B3LYP/6-31G(d) and B3LYP/6-311++G(d,p) levels of theory. The long-range solvent effects on the geometrical and energy parameters of tautomerization were also analyzed by use of the PCM model. The calculated relative Gibbs free energies were used to estimate the equilibrium constants. It was shown that the keto forms are more stable than the enol tautomers both in the gas phase and in solution. The activation energies of tautomerization increase in the following order: lactim–lactam, keto–enol, and imine–enamine transformations. Proton transfer in the solvated complexes and dimers is virtually effortless in relation to that in the isolated tautomers. The bulk of solvent does not substantially affect either the activation energies or the equilibrium constants. The differences between the tautomerism in 4-methyl-1,3-dihydro-2*H*-1,5-benzodiazepin-2-one and in 4-methyl-1,3-dihydro-2*H*-1,5-benzodiazepine-2-thione are discussed.

Introduction

The recent considerable progress in the development of the chemistry of 1,5-benzodiazepin-2-ones and 1,5-benzodiazepine-2-thiones (Scheme 1) is due to the discovery of their valuable pharmacological properties. Among the members of this class there are compounds that display analgesic, anticonvulsive, antiagressive, psychotropic, and antiproliferative activities.[1–3] Molecules containing the 1,5-benzodiazepin-2-one scaffold are privileged substructures exhibiting a range of biological activities, including as interleukin-1β converting enzyme (ICE) inhibitors and as delayed rectifier potassium current blockers.[4] Substituted dihydro-1,5-benzodiazepin-2-ones and dihydro-1,5-benzodiazepine-2-thiones are used as starting materials in the synthesis of several heterocyclic compounds studied for potential biological activities.[5]

There are three kinds of tautomerization for dihydro-1,5-benzodiazepin-2-ones [C(3)–H keto form $\mathbf{1_o}$] resulting from the presence of two nitrogen atoms and a carbonyl group in a seven-membered ring (see Scheme 1): lactim–lactam [leads to C(3)–H enol form $\mathbf{2_o}$], keto–enol [leads to N(1)–H enol form $\mathbf{3_o}$], and imine–enamine [leads to N(5)–H keto form $\mathbf{4_o}$]. As is known, processes involving proton transfer between interconversion tautomers are of fundamental importance in chemistry, in particular in many biochemical reactions. The tautomerization of a reactant is in some cases the necessary condition for exhibition of biological activity.[6] Only a few experimental studies on the tautomerization of substituted dihydro-1,5-benzodiazepin-2-ones and dihydro-1,5-benzodiazepine-2-thiones have been performed.[7–11] The IR spectra of 1,3-dihydro-1,5-benzodiazepin-2-ones reveal that the bands associated with free and associated NH groups appear in the 3400–3160 cm^{-1} region, whereas intensive carbonyl absorption bands (amide I) are observed at 1695–1668 cm^{-1}, together with stretching vibration bands of C=N bonds at 1650–1635 cm^{-1}.[11b] UV spectra of 1,3-dihydro-1,5-benzodiazepin-2-ones exhibited bands associated with the carbonyl group, the NH–Ph aniline group, and the C=N group adjacent to the benzene ring (for 4-methyl-1,3-dihydro-1,5-benzodiazepin-2-one the bands are about 214, 271, and 297 nm).[12] No enol form was observed in solution in a ^1H NMR spectrum of 4-phenyl-1,3-dihydro-2*H*-1,5-benzodiazepin-2-one.[7] It could be concluded from the IR, UV, and ^1H NMR spectra that 1,3-dihydro-2*H*-1,5-benzodiazepin-2-ones might exist in

[a] Department of Organic Chemistry, Dnipropetrovsk National University,
Dnipropetrovsk 49010, Ukraine
Fax: +38-056-374-98-41
E-mail: sokovyty@icnanotox.org
[b] Interdisciplinary Nanotoxicity Center, Department of Chemistry, Jackson State University,
Jackson, Mississippi 39217, USA
[c] Department of Chemistry, Kirovograd State Pedagogical University,
Kirovograd 25006, Ukraine

Supporting information for this article is available on the WWW under http://dx.doi.org/10.1002/ejoc.200900689.

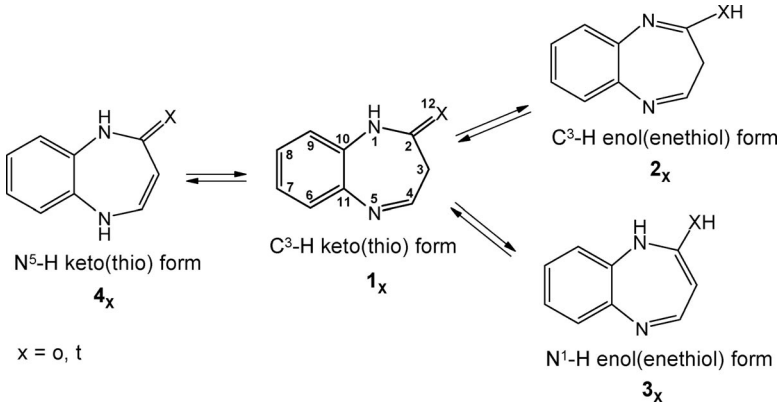

Scheme 1. Tautomers of 1,3-dihydro-2*H*-1,5-benzodiazepin-2-ones and 1,3-dihydro-2*H*-1,5-benzodiazepine-2-thiones.

their C(3)–H keto forms in the solid state and in solution. Kurasawa et al.[8] isolated two stable 3-quinoxalinyl-1,5-benzodiazepin-2-one tautomers, the spectral evidences of which were measured independently. Interestingly, the N(5)–H keto tautomer exhibits reactivity significantly different from that of the C(3)–H keto tautomer. Furthermore, the N(5)–H tautomer was sufficiently stable in the solid state and solution to allow its spectroscopic data to be recorded, and it did not easily isomerize into the C(3)–H tautomer without being heated in acetic acid at reflux. It was demonstrated by one of us on the basis of IR, UV, and ^{1}H NMR spectra that 1,3-dihydro-1,5-benzodiazepine-2-thiones exist primarily in their thione forms in solutions of different polarities.[11c] Nardi et al.[11a] observed the presence of peaks suggesting the presence of N(5)–H thione tautomers together with the C(3)–H thione forms in NMR spectra of some 4-aryl-1,3-dihydro-2*H*-1,5-benzodiazepine-2-thiones. The presence of tautomers and the ratios of these tautomeric forms depend on the solvent used and on the time during which the sample has been in solution. The greater the length of time the sample has been in solution, the more abundant is the N(5)–H tautomer. There are many reported examples of tautomerism in 1,5-aryldiazepin-2-one ring systems in which most of the compounds exist predominately as their C(3)–H keto forms rather than as their N(5)–H keto forms.[13]

To the best of our knowledge, there are no theoretical studies relating to the relative stabilities of tautomers of dihydro-1,5-benzodiazepin-2-ones or their thio analogues, nor of their intramolecular proton-transfer processes. For this study we have therefore investigated tautomeric rearrangements of 4-methyl-1,3-dihydro-2*H*-1,5-benzodiazepin-2-one and 4-methyl-1,3-dihydro-2*H*-1,5-benzodiazepine-2-thione by use of the B3LYP functional in the DFT approach. A few studies of tautomerism of heterocyclic compounds by different quantum chemical methods have been carried out recently.[14,15] The authors[14] have shown that the commonly used B3LYP method provides the correct molecular geometries, activation energies, and energy differences between pairs of tautomers, similarly to MP2-level predictions. They concluded that the small absolute errors and the cost-effectiveness of the computations make the B3LYP method a good choice for these systems.

Many reactions involving benzodiazepinones and benzodiazepinethiones have been carried out both in alcohol and in aprotic solutions.[5,16] As is known, reductions in activation energies of tautomerization caused by multiple hydrogen bond formation are common in many systems.[15,17–19] Proton-transfer in an ethanol solution is mainly governed by the assistance of solvent molecules, so in this study ethanol-assisted proton transfer reactions modeled by explicit consideration of one or two ethanol molecules were compared with intramolecular proton migration. In an aprotic solution self-mediated proton transfer may take place, so self-assisted tautomerization is also examined.

On the basis of the results of these calculations, the relative stability orders of the isolated, solvated, and dimeric tautomeric forms of 4-methyl-1,3-dihydro-2*H*-1,5-benzodiazepin-2-one and 4-methyl-1,3-dihydro-2*H*-1,5-benzodiazepine-2-thione, their proton-transfer reactions, and the effect of polar solvents on the above phenomena are discussed.

Results and Discussion

The geometries of the tautomers and transition states for the tautomerization of isolated and monosolvated complexes of the 4-methyl-1,3-dihydro-2*H*-1,5-benzodiazepin-2-one and the 4-methyl-1,3-dihydro-2*H*-1,5-benzodiazepine-2-thione were optimized at the B3LYP/6-311++G(d,p) level.[20] All geometries of local minima and transition states were optimized without any symmetry restrictions. Stationary points were further characterized as minima (with all real frequencies) or as transition states (with only one imaginary frequency) by computations of analytic harmonic vibrational frequencies at the same theory level as geometry optimization. Long-range solvent effects were taken into account by use of the PCM[21] method to determine the solvent effects on the geometric and energetic parameters of the studied species and the tautomerization re-

action processes. For disolvated and dimeric complexes the geometry optimization and frequency analysis were performed at the B3LYP/6-31G(d) level, whereas single-point energies were calculated at the B3LYP/6-311++G(d,p)//B3LYP/6-31G(d) and PCM/B3LYP/6-311++G(d,p)//B3LYP/6-31G(d) levels. Transition state structures for all studied catalytic tautomerization processes in 4-methyl-1,3-dihydro-2*H*-1,5-benzodiazepin-2-one were checked by intrinsic reaction coordinate (IRC) computations[22] at the same level of theory. The total energies were corrected for the zero-point energies and for thermal and entropic contributions at 298.15 K calculated at the same levels of theory as were used for optimization. The zero-point energies were scaled by a factors of 0.9806[23] at the B3LYP/6-31G(d) level. All calculations were carried out with the Gaussian 03 program package.[24]

The following notations for the tautomers of 4-methyl-1,3-dihydro-2*H*-1,5-benzodiazepin-2-one and its sulfur analogue are employed throughout this work (Scheme 2). Benzodiazepin-2-ones and benzodiazepine-2-thiones are denoted by "o" (one) or "t" (thione) subscripts. The 4-methyl-1,3-dihydro-2*H*-1,5-benzodiazepin-2-one (**1**$_o$) molecule is characterized by the presence of three labial protons and two distinct sites to which they can be attached. Structures **2**$_o$ and **3**$_o$ are formed by transfer of the amino or the methylene group's proton to the O(12) site. Structure **4**$_o$ is obtained through proton transfer from the methylene group to the N(5) site.

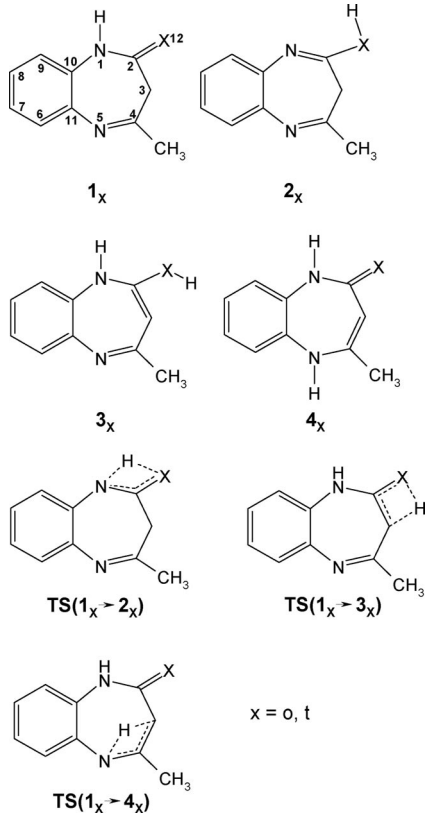

Scheme 2. Tautomers and transition state structures for intramolecular proton transfer of 4-methyl-1,3-dihydro-2*H*-1,5-benzodiazepin-2-one and 4-methyl-1,3-dihydro-2*H*-1,5-benzodiazepine-2-thione.

The manuscript is arranged in the following order: proton transfer through an intramolecular mechanism, a mechanism involving one ethanol molecule as a bifunctional catalyst in an intermediate cyclic structure, a mechanism involving two bridged ethanol molecules, tautomeric interconversion within a self-associated dimer, and, finally, comparison of the tautomerism of 4-methyl-1,3-dihydro-2*H*-1,5-benzodiazepin-2-one with that of 4-methyl-1,3-dihydro-2*H*-1,5-benzodiazepine-2-thione. The bulk solvent effects on the kinetics and the thermodynamics of the tautomerization reactions are discussed with comparison with the gas-phase results through the text.

Schemes 2, 4, 5, and 6 show schematic representations of the reactants, transition states, and products involved in the direct, monoethanol-assisted, diethanol-assisted, and self-assisted proton-transfer reactions for 4-methyl-1,3-dihydro-2*H*-1,5-benzodiazepin-2-one and 4-methyl-1,3-dihydro-2*H*-1,5-benzodiazepine-2-thione. The energy parameters of the tautomerizations are listed in Tables 1, 2, 3, 4, 5, 6, 7, and 8 in the text and in Tables S1–S4 in the Supporting Information. The molecular geometries calculated for all structures in the gas phase are listed in Tables S5–S14 in the Supporting Information. Figures S1–S10 (Supporting Information) demonstrate an evaluation of bond lengths and energy changes by IRC calculations for the tautomerization of the 4-methyl-1,3-dihydro-2*H*-1,5-benzodiazepin-2-one.

Intramolecular Proton Transfer

A schematic representation of the tautomers and transition state structures for intramolecular proton transfers is shown in Scheme 2 and the calculated geometric data are listed in Tables S5 and S7 (see the Supporting Information). The calculated relative Gibbs free energies and the dipole moments of the tautomers of 4-methyl-1,3-dihydro-2*H*-1,5-benzodiazepin-2-one are listed in Table 1. From the presented data, it is clear that the keto form **1**$_o$ is the most stable one in the gas phase whereas the keto form **4**$_o$ emerges as the next most stable form. The most stable structures each possess an intramolecular hydrogen bond that appears to be stronger in the keto forms. The energy difference between the two most stable tautomers **1**$_o$ and **4**$_o$ in the gas phase is 3.49 kcal mol^{-1}. The **3**$_o$ and **2**$_o$ forms are located at 22.32 and 11.59 kcal mol^{-1}, respectively, above the **1**$_o$ tautomer on the potential energy surface. Therefore, the following relative stability order of the tautomeric structures of 4-methyl-1,3-dihydro-2*H*-1,5-benzodiazepin-2-one is predicted: **1**$_o$ > **4**$_o$ > **2**$_o$ > **3**$_o$. In view of the high relative energies of the **2**$_o$ and **3**$_o$ tautomers one can conclude that they should not be observed in the gas phase. The energy/reaction path plot for tautomeric transformations of 4-methyl-1,3-dihydro-2*H*-1,5-benzodiazepin-2-one in the gas phase is shown in Scheme 3.

Table 1. Calculated [B3LYP/6-311++G(d,p) and PCM/B3LYP/6-311++G(d,p) levels] relative Gibbs free energies (ΔG, kcal mol^{-1}, 298.15 K) for 4-methyl-1,3-dihydro-2*H*-1,5-benzodiazepin-2-one tautomers and free energy barriers[a] [kcal mol^{-1}] for intramolecular tautomerization.

Structure	D	ΔG_{gas}	ΔG_{et}
$\mathbf{1_o}$	2.32	0.00	0.00
$\mathbf{4_o}$	5.21	3.49	0.14
$\mathbf{2_o}$	1.81	11.59	12.27
$\mathbf{3_o}$	3.09	22.32	18.41
TS($\mathbf{1_o}$→$\mathbf{2_o}$)	1.96	41.99	47.10
TS($\mathbf{1_o}$→$\mathbf{3_o}$)	1.81	60.39	61.10
TS($\mathbf{1_o}$→$\mathbf{4_o}$)	4.24	73.77	74.22

[a] Because the relative energies of the transition states are listed relative to structure $\mathbf{1_o}$ these values correspond to the free energy barrier for its tautomerization.

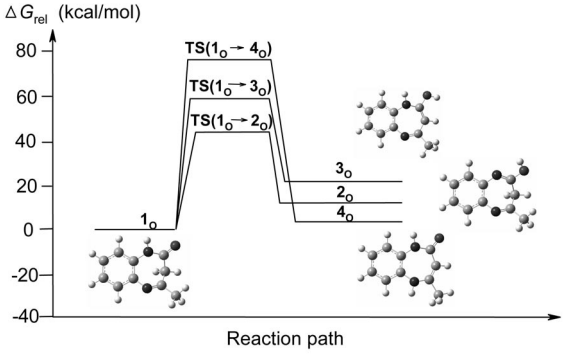

Scheme 3. Plot of energy/reaction path for tautomeric transformations of 4-methyl-1,3-dihydro-2*H*-1,5-benzodiazepin-2-one in the gas phase.

As can be seen from Table 1, the calculated dipole moments for tautomers $\mathbf{1_o}$, $\mathbf{4_o}$, $\mathbf{2_o}$, and $\mathbf{3_o}$ are 2.32, 5.21, 1.81, and 3.09 D, respectively. Accordingly, the $\mathbf{3_o}$ and $\mathbf{4_o}$ tautomers would be predicted to be the most solvated species. Their relative energies are lower than the corresponding gas-phase values by 3.91 and 3.35 kcal mol^{-1}, respectively, whereas the relative energy for $\mathbf{2_o}$ is higher by 0.68 kcal mol^{-1}. This means that in solution the populations of the $\mathbf{3_o}$ and $\mathbf{4_o}$ tautomers should be higher, while the populations of $\mathbf{2_o}$ and $\mathbf{1_o}$ tautomers should be lower than under gas-phase conditions.

We concluded that the $\mathbf{1_o}$ and $\mathbf{4_o}$ tautomers have virtually the same stability. This confirms the existence of both keto tautomers observed in experimental studies of substituted 1,5-benzodiazepin-2-ones.[8]

From the values of the Gibbs free energies for intramolecular tautomerizations (see Table 1) one can see that intramolecular proton transfers are characterized by high free energies. The proton transfer for $\mathbf{1_o}$→$\mathbf{2_o}$ tautomerization is the most favorable, with a free energy barrier of 41.99 kcal mol^{-1}, and differs significantly from the other transformations because the N–H bond dissociation energy has a smaller value than that for the C–H bond. This is in good agreement with results computed at the MP2/6-31+G(d,p) level for 5-fluorouracil,[25] but the values for pyridone,[15] cytosine,[18] and hypoxanthine[19] obtained at the MP2 level with use of different basis sets are relatively low (34–35 kcal mol^{-1}). The C=O group has better polarity and proton acceptor ability than the C=N group, so the free energy barrier for $\mathbf{1_o}$→$\mathbf{3_o}$ proton transfer (60.39 kcal mol^{-1}) is lower than that for the $\mathbf{1_o}$→$\mathbf{4_o}$ transformation (73.77 kcal mol^{-1}). The high value of free energy for the $\mathbf{1_o}$→$\mathbf{4_o}$ tautomerization is consistent with those for imine–enamine tautomerization in α-substituted acetaldimines.[26] The effect of a dielectric solvent on the free energies of **TS($\mathbf{1_o}$→$\mathbf{4_o}$)** and **TS($\mathbf{1_o}$→$\mathbf{3_o}$)** transition states is negligible (changes are smaller than 1 kcal mol^{-1}). However, the free energy barrier for $\mathbf{1_o}$→$\mathbf{2_o}$ transformation in solution is higher than in the gas phase, by 5.11 kcal mol^{-1}.

A proton is much lighter than other atoms, and delocalization paths (by quantum tunneling) that involve motion of the solute while the solvent structure is kept frozen may exist. We calculated tunneling corrections as a way to reduce high classical energy barriers with the aid of the simplest Wigner transformation coefficient,[27] given by $K(T) = 1 + (\hbar|\omega|/kT)^2/24$. The tunneling correction coefficients for intramolecular tautomerizations examined here are small and vary between 1.00 and 1.10 at a temperature of 298.15 K. This clearly shows that tunneling has virtually no influence on the rate constant of intramolecular proton transfer for 4-methyl-1,3-dihydro-2*H*-1,5-benzodiazepin-2-one.

As is known, proton transfer processes that take place between two species stabilized by intermolecular hydrogen bonds generally exhibit much lower free energy barriers to tautomerization,[15,17–19] so the formation either of complexes with ethanol molecules or of dimers might provide energetically accessible pathways for tautomerizations. This is discussed in the next parts of this manuscript.

Ethanol-Assisted Mechanism

A schematic representation of the tautomers and transition state structures for ethanol-assisted proton transfers is shown in Scheme 4 and the calculated geometric data are listed in Table S9 (see the Supporting Information). The calculated relative free energies of the tautomers and free energy barriers for ethanol-assisted tautomerizations are listed in Table 2 together with the dipole moments of the solvated tautomeric complexes and transition state structures. The interaction between an ethanol molecule and isolated tautomers of 4-methyl-1,3-dihydro-2*H*-1,5-benzodiazepin-2-one slightly stabilizes the $\mathbf{2_o}$·**et** and $\mathbf{3_o}$·**et** forms (by approximately 1 kcal mol^{-1}), but destabilizes the $\mathbf{4_o}$·**et** form (by 2.21 kcal mol^{-1}) relative to $\mathbf{1_o}$·**et**[a], as can be seen in Tables 1 and 2. The relative stability sequence for the ethanol-solvated tautomeric complexes of 4-methyl-1,3-dihydro-2*H*-1,5-benzodiazepin-2-one is as follows: $\mathbf{1_o}$·**et** > $\mathbf{4_o}$·**et** > $\mathbf{2_o}$·**et** > $\mathbf{3_o}$·**et**. The inclusion of the bulk electrostatic interaction with a solvent slightly changes the relative stabilities of the tautomeric forms. Because of the larger dipole moments of $\mathbf{4_o}$·**et** and $\mathbf{3_o}$·**et**, both of these forms are more stable in ethanol solution (relative ΔG values lower by 8.82 and

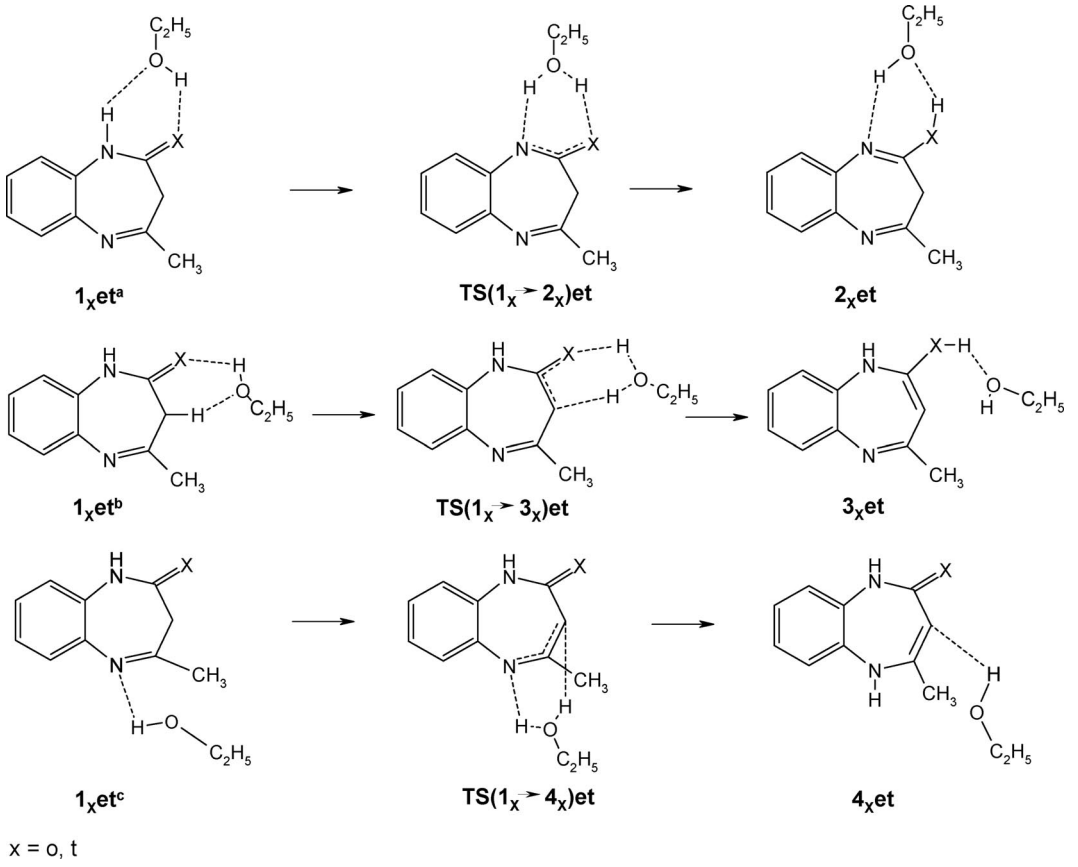

Scheme 4. Solvated complexes of tautomers and transition state structures for monoethanol-assisted proton transfer of 4-methyl-1,3-dihydro-2*H*-1,5-benzodiazepin-2-one and 4-methyl-1,3-dihydro-2*H*-1,5-benzodiazepine-2-thione.

7.65 kcal mol^{-1}, respectively) than in the gas phase. As a result, the **1$_o$·et** and **4$_o$·et** tautomers have virtually the same stability.

Table 2. Calculated [B3LYP/6-311++G(d,p) and PCM/B3LYP/6-311++G(d,p) levels] relative Gibbs free energies (ΔG, kcal mol^{-1}, 298.15 K) of ethanol-solvated complexes of 4-methyl-1,3-dihydro-2*H*-1,5-benzodiazepin-2-one tautomers and transition states, together with free energy barriers [kcal mol^{-1}] for ethanol-assisted tautomerization.

Structure	D	ΔG_{gas}[a]	ΔG_{et}[a]
1$_o$·et^a	0.83	0.00	0.00
TS(1$_o$→2$_o$)·et	2.25	18.91 (18.91)	19.79 (19.79)
2$_o$·et	1.99	10.61	11.73
1$_o$·et^b	2.46	1.03	–3.30
TS(1$_o$→3$_o$)·et	2.94	42.62 (41.59)	39.50 (42.80)
3$_o$·et	6.77	21.42	13.77
1$_o$·et^c	2.65	2.04	–1.23
TS(1$_o$→4$_o$)·et	6.47	56.32 (54.28)	48.55 (49.78)
4$_o$·et	7.64	5.70	–3.12

[a] Relative Gibbs free energies of all structures are given relative to the **1$_o$·et^a** complex. Free energy barriers of reactions are given in parentheses.

As would be expected, the assistance of an ethanol molecule in the proton transfer process greatly reduces the free energy barrier (by approximately 20 kcal mol^{-1}). The free energies for tautomerizations of **1$_o$·et^a→2$_o$·et**, **1$_o$·et^b→3$_o$·et**, and **1$_o$·et^c→4$_o$·et** are 18.91, 41.59, and 54.28 kcal mol^{-1}, respectively. The ethanol-assisted proton transfer process is characterized by smaller free energy barrier because it is carried out through a six-membered-ring transition state, which has a lower ring strain than the four-membered-ring transition state in the case of the intramolecular process. From Table 2 one can see that inclusion of the bulk electrostatic interactions slightly increases the free energy barriers (about 1 kcal mol^{-1}) for the **1$_o$·et^a→2$_o$·et** and **1$_o$·et^b→3$_o$·et** tautomerizations but reduces the free energy (about 4.5 kcal mol^{-1}) for the **1$_o$·et^c→4$_o$·et** transformation. The calculated value of free energy for the **1$_o$·et^a→2$_o$·et** tautomerization is close to the values found recently for water-assisted keto–enol tautomerization for pyridone[15] and 5-fluorouracil.[25]

Diethanol-Assisted Mechanism

A schematic representation of the tautomers and transition state structures for diethanol-assisted proton transfers is shown in Scheme 5 and the calculated geometric data are listed in Table S11 (see the Supporting Information). The energy parameters and dipole moments of all the forms of diethanol-solvated complexes involved in diethanol-assisted tautomerization are listed in Table 3. The relative free energies for the disolvated complexes **2$_o$·et$_2$**, **3$_o$·et$_2$**, and **4$_o$·et$_2$** are higher than those of the corresponding monosolvated

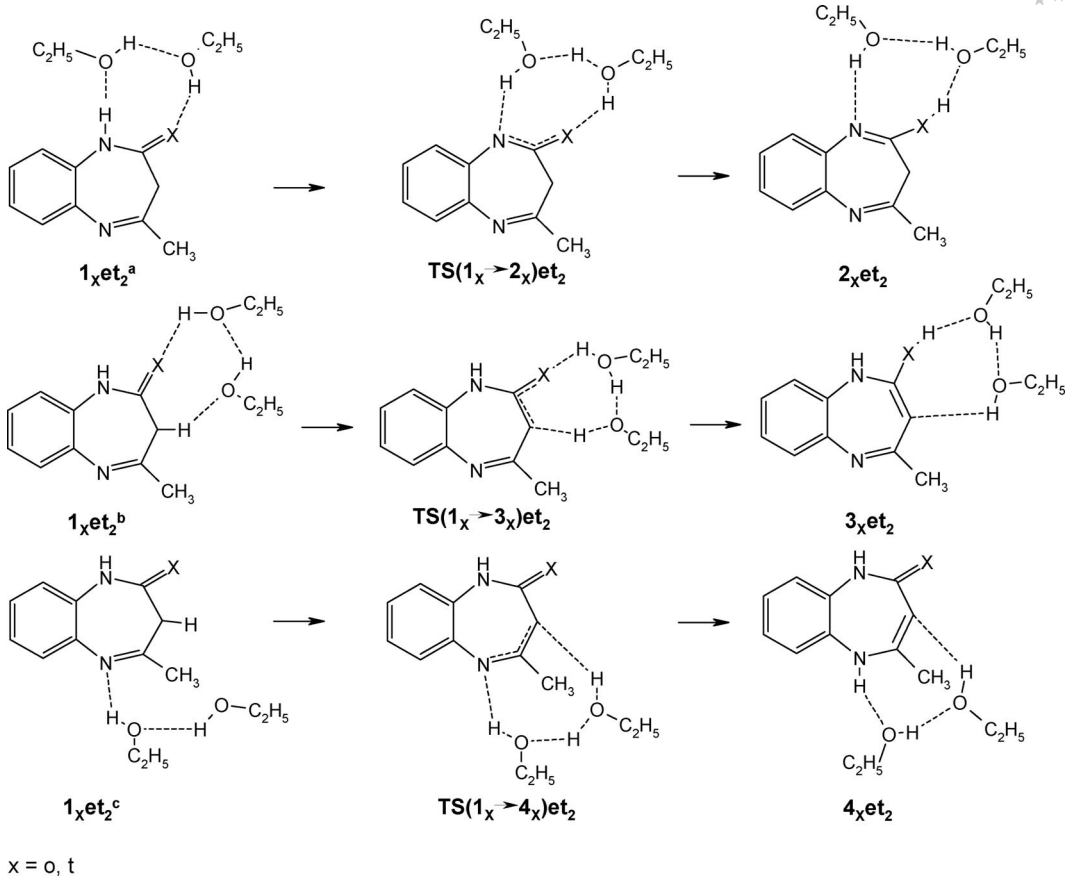

Scheme 5. Solvated complexes of tautomers and transition state structures for diethanol-assisted proton transfer of 4-methyl-1,3-dihydro-2*H*-1,5-benzodiazepin-2-one and 4-methyl-1,3-dihydro-2*H*-1,5-benzodiazepine-2-thione.

complexes by 0.78, 2.03 and 3.93 kcal mol^{-1}, respectively. These changes may be explained in terms of the formation of stronger hydrogen bonds in the $\mathbf{1_o{\cdot}et_2^a}$ and $\mathbf{2_o{\cdot}et_2}$ complexes than in the $\mathbf{3_o{\cdot}et_2}$ and $\mathbf{4_o{\cdot}et_2}$ complexes (see Table S11 in the Supporting Information). Therefore, disolvation shifts the tautomeric equilibrium towards the $\mathbf{1_o{\cdot}et_2^a}$ keto form, which substantially dominates for such species. The relative stability order of these four diethanol-solvated complexes is similar to those for isolated and monosolvated species. The bulk of the ethanol stabilizes the $\mathbf{4_o{\cdot}et_2}$ and $\mathbf{3_o{\cdot}et_2}$ complexes more significantly, which is consistent with their larger dipole moments (see Table 3). The equilibrium concentrations of the tautomers therefore change, but the stability order in solution remains the same as in the gas phase.

The available literature data for keto–enol tautomerization assisted by two bridged water molecules indicate that the second water molecule in the bridging site has no significant effect on the reduction of the activation energy, relative to the monohydration process.[15,19] As can be seen from Tables 2 and 3, further inclusion of one more ethanol molecule located as a bridge between the N(1)–H(1) and C(2)=O(12) sites yields, as would be expected, a free energy barrier of 17.27 kcal mol^{-1} for $\mathbf{1_o{\cdot}et_2^a \rightarrow 2_o{\cdot}et_2}$ tautomerization, slightly different from the barrier of the corresponding monoethanol-assisted tautomerization (18.91 kcal mol^{-1}). Although the effect of the second ethanol molecule in the bridging site on the kinetics of the $\mathbf{1_o{\cdot}et_2^a \rightarrow 2_o{\cdot}et_2}$ tautomerization is not significant, disolvation substantially reduces the free energies for $\mathbf{1_o{\cdot}et_2^c \rightarrow 4_o{\cdot}et_2}$ (by 18.13 kcal mol^{-1}) and for $\mathbf{1_o{\cdot}et_2^b \rightarrow 3_o{\cdot}et_2}$ (by 10.70 kcal mol^{-1}) tautomerizations. When long-range effects of ethanol solvent are additionally taken into account all three free energy barriers are slightly decreased, relative to the gas phase.

Table 3. Calculated [B3LYP/6-311++G(d,p)//B3LYP/6-31G(d) and PCM/B3LYP/6-311++G(d,p)//B3LYP/6-31G(d) levels] relative Gibbs free energies (ΔG, kcal mol^{-1}, 298.15 K) of diethanol-solvated complexes of 4-methyl-1,3-dihydro-2*H*-1,5-benzodiazepin-2-one tautomers and transition states, together with free energy barriers [kcal mol^{-1}] for diethanol-assisted tautomerization.

Structure	D	ΔG_{gas}[a]	ΔG_{et}[a]
$\mathbf{1_o{\cdot}et_2^a}$	1.26	0.00	0.00
$\mathbf{TS(1_o{\rightarrow}2_o){\cdot}et_2}$	2.05	17.27 (17.27)	17.17 (17.17)
$\mathbf{2_o{\cdot}et_2}$	0.92	11.39	12.04
$\mathbf{1_o{\cdot}et_2^b}$	1.55	4.93	0.70
$\mathbf{TS(1_o{\rightarrow}3){\cdot}et_2}$	5.98	35.82 (30.89)	30.08 (29.38)
$\mathbf{3_o{\cdot}et_2}$	3.87	23.45	19.91
$\mathbf{1_o{\cdot}et_2^c}$	3.24	5.80	0.30
$\mathbf{TS(1_o{\rightarrow}4_o){\cdot}et_2}$	7.31	41.95 (36.15)	34.06 (33.76)
$\mathbf{4_o{\cdot}et_2}$	4.80	9.63	4.69

[a] Gibbs free energies of all structures are relative to the $\mathbf{1_o{\cdot}et_2^a}$ complex. Free energy barriers of reactions are given in parentheses.

In conclusion, these results suggest that proton transfer for the three types of tautomerization discussed in this study should be facilitated by the presence of one or two ethanol molecules.

Self-Assisted Mechanism

The $\mathbf{1_o}$ monomer could form several dimers. We have chosen four of them characterized by high stability [$(\mathbf{1_o})_2$[a] – $(\mathbf{1_o})_2$[d]]. Double proton transfer in these dimers leads to the formation of new dimers, which may dissociate to form $\mathbf{3_o}$, $\mathbf{2_o}$, or $\mathbf{4_o}$ monomers or mixtures (see Scheme 6). The relative energies of the dimers and the activation energies for interconversion of dimers are listed in Table 4. The most stable dimer in the gas phase $(\mathbf{1_o})_2$[a] features two intermolecular N–H···O=C hydrogen bonds. This is consistent with data for tetrahydro-1,5-benzodiazepin-2-ones and dihydro-1,4-benzodiazepin-2-ones, which are stabilized in their crys-

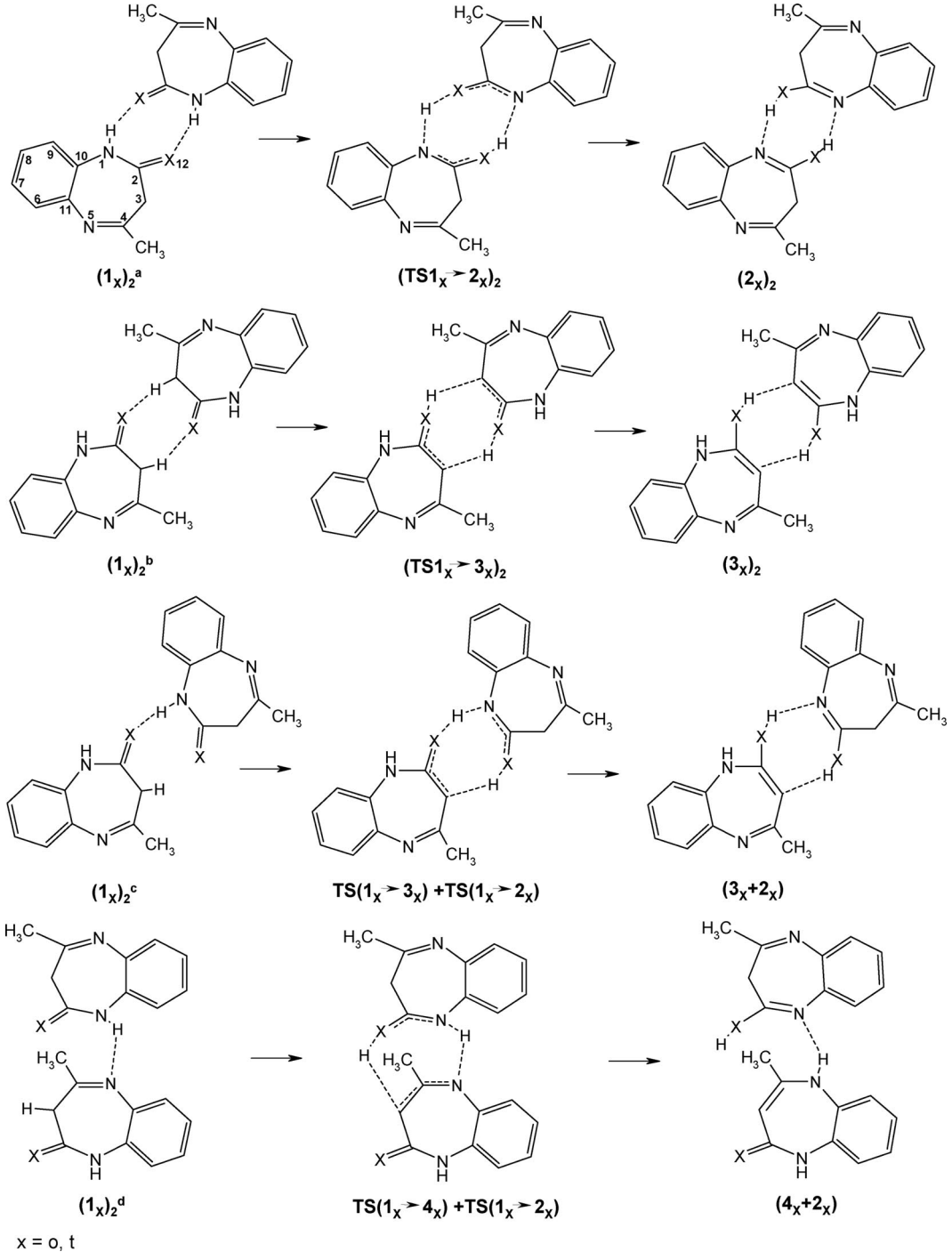

Scheme 6. Dimers and transition state structures for self-assisted proton transfer of 4-methyl-l,3-dihydro-2*H*-1,5-benzodiazepin-2-one and 4-methyl-l,3-dihydro-2*H*-1,5-benzodiazepine-2-thione.

tal packing by N–H···O=C hydrogen bonds.[28] The existence in the IR spectra of bands corresponding to associated NH group stretching vibrations suggests that 2,3-dihydro-1,5-benzodiazepin-2-ones and their thio analogues may exist in nonpolar solvents in dimeric forms through the formation of intermolecular hydrogen bonds involving their N–H groups.[11,12]

Table 4. Calculated [B3LYP/6-311++G(d,p)//B3LYP/6-31G(d) and PCM/B3LYP/6-311++G(d,p)//B3LYP/6-31G(d) levels] relative Gibbs free energies (ΔG, kcal mol^{-1}, 298.15 K) of dimers of 4-methyl-1,3-dihydro-2*H*-1,5-benzodiazepin-2-one and transition states, together with free energy barriers [kcal mol^{-1}] for self-assisted tautomerization.

Structure	D	ΔG_{gas}[a]	ΔG_{ac}[a]
$(\mathbf{1_o})_2$[a]	2.13	0.00	0.00
$[\mathbf{TS(1_o \rightarrow 2_o)}]_2$	1.74	16.09	17.16
$(\mathbf{2_o})_2$	1.72	18.11	19.38
$(\mathbf{1_o})_2$[b]	1.80	8.20	–0.08
$[\mathbf{TS(1_o \rightarrow 3_o)}]_2$	3.35	61.09 (52.88)	52.49 (52.57)
$(\mathbf{3_o})_2$	1.36	54.00	46.43
$(\mathbf{1_o})_2$[c]	1.77	3.65	–0.47
$\mathbf{TS(1_o \rightarrow 3_o)} + \mathbf{TS(1_o \rightarrow 2_o)}$	5.00	38.07 (34.42)	33.75 (34.22)
$\mathbf{(3_o + 2_o)}$	3.62	36.48	33.35
$(\mathbf{1_o})_2$[d]	3.44	7.17	–0.59
$\mathbf{TS(1_o \rightarrow 4_o)} + \mathbf{TS(1_o \rightarrow 2_o)}$	7.91	47.21 (40.05)	39.93 (40.52)
$\mathbf{(4_o + 2_o)}$	4.63	20.54	15.21

[a] Gibbs free energies of all structures are relative to the $(\mathbf{1_o})_2$[a] dimer. Free energy barriers of reactions are given in parentheses.

Interestingly, the relative energy of the transition state $[\mathbf{TS(1_o \rightarrow 2_o)}]_2$ is lower than that of the $(\mathbf{2_o})_2$ dimer (see Table 4), so the free energy for the transformation $(\mathbf{1_o})_2^{a} \rightarrow (\mathbf{2_o})_2$ is 18.11 kcal mol^{-1}. Similar results have been found for the keto–enol tautomerization of imidazolidin-4-one,[6] for which a transition state calculated at the CPCM/B3LYP/6-311++G(2d,p) level of theory is located at 12.05 kcal mol^{-1}, whereas the relative energy of the enol tautomer amounts to 18.80 kcal mol^{-1}. By comparison of activation barriers for the $(\mathbf{1_o})_2^{b} \rightarrow (\mathbf{3_o})_2$ and $(\mathbf{1_o})_2^{c} \rightarrow (\mathbf{3_o + 2_o})$ tautomerizations one may conclude that the second process is more favorable for formation of the $\mathbf{3_o}$ tautomer. Note that this pathway is also characterized by a lower free energy barrier (by 25.97 kcal mol^{-1}) than the intramolecular $\mathbf{1_o \rightarrow 3_o}$ tautomerization. The self-assisted mechanism decreases the free energy barrier for imine–enamine tautomerization to 40.05 kcal mol^{-1}, in comparison with the free energy of 73.77 kcal mol^{-1} seen for the intramolecular mechanism. The inclusion of long-range effects of acetone as solvent changes the predicted free energy barriers slightly (about 1 kcal mol^{-1}). All the results indicate that the cyclic dimers of $(\mathbf{1_o})_2^{a}$–$(\mathbf{1_o})_2^{d}$ assist acceleration of the proton transfer. In all cases, the reactant dimers are more stable than the corresponding product dimers.

The general picture emerging from the above computations indicates that the high energy barrier rules out the possibility of intramolecular proton-transfer reactions of 4-methyl-1,3-dihydro-2*H*-1,5-benzodiazepin-2-one in the ground state. Because the $\mathbf{1_o}$ structure possesses both donor and acceptor H-bonding sites, it forms stable dimers and complexes with the other species present, such as ethanol molecules. The formation of a dimer or complex greatly reduces the activation barrier and increases the possibility of tautomerization.

Tautomerism of 4-Methyl-1,3-dihydro-2*H*-1,5-benzodiazepine-2-thione

The above results of calculations of the tautomeric transformations of 4-methyl-1,3-dihydro-2*H*-1,5-benzodiazepin-2-one were compared with those for the tautomerism of 4-methyl-1,3-dihydro-2*H*-1,5-benzodiazepine-2-thione to investigate the energy changes caused by substitution of oxygen by sulfur. Because of the structural similarity of 4-methyl-1,3-dihydro-2*H*-1,5-benzodiazepin-2-one and 4-methyl-1,3-dihydro-2*H*-1,5-benzodiazepine-2-thione we expected that the tautomerism should generally be the same in both series, so our main goal here is discussion of the differences in tautomerization processes for these compounds.

Sulfur is less electronegative than oxygen, the lone-pair electrons of sulfur are more polarizable, and sulfur is more π-donating and hence stabilizes the $\mathbf{2_t}$ and $\mathbf{3_t}$ enethiol forms and $\mathbf{TS(1_t \rightarrow 2_t)}$ and $\mathbf{TS(1_t \rightarrow 3_t)}$ transition states more strongly than oxygen. As can be seen from Tables 1 and 5, the relative free energies of the $\mathbf{2_t}$ and $\mathbf{3_t}$ tautomers are lower (by 3.30 and 5.71 kcal mol^{-1}, respectively) than those of the $\mathbf{2_o}$ and $\mathbf{3_o}$ tautomers. Substitution of oxygen by sulfur thus diminishes the energy difference between isolated tautomeric forms but maintains the order of their relative stabilities. As can be seen by comparison of the corresponding data, shown in Tables 1, 2, 3, 4, 5, 6, 7, and 8, the relative free energies of the isolated, monosolvated, disolvated, and dimeric forms of the $\mathbf{3_t}$ and $\mathbf{4_t}$ tautomers are smaller than those of their oxo analogues both in the gas phase and in solution. The relative free energies of the isolated, monosolvated forms of the $\mathbf{2_t}$ tautomer are smaller than those predicted for the $\mathbf{2_o}$ tautomer, whereas for the disolvated and dimeric forms of these tautomers the reverse trend is observed.

Table 5. Calculated [B3LYP/6-311++G(d,p) and PCM/B3LYP/6-311++G(d,p) levels] relative Gibbs free energies (ΔG, kcal mol^{-1}, 298.15 K) of 4-methyl-1,3-dihydro-2*H*-1,5-benzodiazepine-2-thione tautomers and free energy barriers[a] [kcal mol^{-1}] for intramolecular tautomerization.

Structure	D	ΔG_{gas}	ΔG_{et}
$\mathbf{1_t}$	3.27	0.00	0.00
$\mathbf{4_t}$	6.18	2.15	–1.79
$\mathbf{2_t}$	1.70	8.29	10.82
$\mathbf{3_t}$	1.99	16.61	15.79
$\mathbf{TS(1_t \rightarrow 2_t)}$	2.25	33.15	38.83
$\mathbf{TS(1_t \rightarrow 3_t)}$	1.61	52.83	53.62
$\mathbf{TS(1_t \rightarrow 4_t)}$	5.26	74.76	74.54

[a] Because the energies of transition states are relative to the $\mathbf{1_t}$ structure these values correspond to the free energy barrier for its tautomerization.

The free energy of the $\mathbf{1_t \rightarrow 2_t}$ tautomerization is smaller than the energy of the $\mathbf{1_o \rightarrow 2_o}$ tautomerization, by 8.84 and 8.27 kcal mol^{-1} for gas phase and ethanol solution, respec-

Table 6. Calculated [B3LYP/6-311++G(d,p) and PCM/B3LYP/6-311++G(d,p) levels] relative Gibbs free energies (ΔG, kcal mol^{-1}, 298.15 K) of ethanol-solvated complexes of 4-methyl-1,3-dihydro-2*H*-1,5-benzodiazepine-2-thione tautomers and transition states, together with free energy barriers [kcal mol^{-1}] for ethanol-assisted tautomerization.

Structure	D	ΔG_{gas}[a]	ΔG_{et}[a]
$\mathbf{1_t \cdot et^a}$	1.89	0.00	0.00
$\mathbf{TS(1_t \rightarrow 2_t) \cdot et}$	2.81	18.97 (18.97)	19.48 (19.48)
$\mathbf{2_t \cdot et}$	1.94	10.40	11.13
$\mathbf{1_t \cdot et^b}$	2.83	2.09	–1.86
$\mathbf{TS(1_t \rightarrow 3_t) \cdot et}$	4.15	41.84 (39.75)	36.57 (38.43)
$\mathbf{3_t \cdot et}$	5.07	19.93	12.59
$\mathbf{1_t \cdot et^c}$	3.26	2.23	–0.94
$\mathbf{TS(1_t \rightarrow 4_t) \cdot et}$	7.18	54.76 (52.53)	46.23 (47.17)
$\mathbf{4_t \cdot et}$	5.52	5.51	–3.20

[a] Gibbs free energies of all structures are relative to the $\mathbf{1_t \cdot et^a}$ complex. Free energy barriers of reactions are given in parentheses.

Table 7. Calculated [B3LYP/6-311++G(d,p)//B3LYP/6-31G(d) and PCM/B3LYP/6-311++G(d,p)//B3LYP/6-31G(d) levels] relative Gibbs free energies (ΔG, kcal mol^{-1}, 298.15 K) of diethanol-solvated complexes of 4-methyl-1,3-dihydro-2*H*-1,5-benzodiazepine-2-thione tautomers and transition states, together with free energy barriers [kcal mol^{-1}] for diethanol-assisted tautomerization.

Structure	D	ΔG_{gas}[a]	ΔG_{et}[a]
$\mathbf{1_t \cdot et_2^a}$	1.53	0.00	0.00
$\mathbf{TS(1_t \rightarrow 2_t) \cdot et_2}$	2.84	18.43 (18.43)	17.25 (17.25)
$\mathbf{2_t \cdot et_2}$	1.69	12.59	13.47
$\mathbf{1_t \cdot et_2^b}$	1.00	3.20	–1.98
$\mathbf{TS(1_t \rightarrow 3_t) \cdot et_2}$	6.98	34.31 (31.11)	26.47 (28.45)
$\mathbf{3_t \cdot et_2}$	3.03	21.64	18.55
$\mathbf{1_t \cdot et_2^c}$	3.99	4.90	–0.59
$\mathbf{TS(1_t \rightarrow 4_t) \cdot et_2}$	7.98	38.17 (33.27)	29.42 (30.01)
$\mathbf{4_t \cdot et_2}$	5.99	6.46	0.86

[a] Gibbs free energies of all structures are relative to the $\mathbf{1_t \cdot et_2^a}$ complex. Free energy barriers of reactions are given in parentheses.

Table 8. Calculated [B3LYP/6-311++G(d,p)//B3LYP/6-31G(d) and PCM/B3LYP/6-311++G(d,p)//B3LYP/6-31G(d) levels] relative Gibbs free energies (ΔG, kcal mol^{-1}, 298.15 K) of dimers of 4-methyl-1,3-dihydro-2*H*-1,5-benzodiazepine-2-thione and transition states, together with free energy barriers [kcal mol^{-1}] for self-assisted tautomerization.

Structure	D	ΔG_{gas}[a]	ΔG_{ac}[a]
$\mathbf{(1_t)_2^a}$	1.31	0.00	0.00
$\mathbf{[TS(1_t \rightarrow 2_t)]_2}$	1.34	23.21 (23.21)	24.78 (24.78)
$\mathbf{(2_t)_2}$	1.00	21.06	22.70
$\mathbf{(1_t)_2^b}$	3.36	5.84	–3.50
$\mathbf{[TS(1_t \rightarrow 3_t)]_2}$	5.12	55.24 (49.41)	45.72 (49.22)
$\mathbf{(3_t)_2}$	3.98	39.07	27.95
$\mathbf{(1_t)_2^c}$	1.68	3.80	–1.09
$\mathbf{TS(1_t \rightarrow 3_t)+TS(1_t \rightarrow 2_t)}$	6.31	37.40 (33.60)	33.42 (34.51)
$\mathbf{(3_t+2_t)}$	3.99	30.74	28.74
$\mathbf{(1_t)_2^d}$	4.34	4.01	–1.85
$\mathbf{TS(1_t \rightarrow 4_t)+TS(1_t \rightarrow 2_t)}$	9.68	41.45 (37.44)	33.15 (35.00)
$\mathbf{(4_t+2_t)}$	8.24	15.03	9.44

[a] Gibbs free energies of all structures are relative to the $\mathbf{(1_t)_2^a}$ dimer. Free energy barriers of reactions are given in parentheses.

tively. The free energy barrier values indicate that the substitution of oxygen by sulfur facilitates the intramolecular proton transfer process from N(1) to S(12), relative to the keto form. In contrast, for the self-assisted mechanism the free energy barrier for the $\mathbf{(1_t)_2^a \rightarrow (2_t)_2}$ tautomerization is larger than that for the $\mathbf{(1_o)_2^a \rightarrow (2_o)_2}$ tautomerization. The free energies for the ethanol-assisted $\mathbf{1_t \cdot et^a \rightarrow 2_t \cdot et}$ and $\mathbf{1_t \cdot et_2}^a \rightarrow \mathbf{2_t \cdot et_2}$ tautomerizations are close to those of their oxo analogues. The $\mathbf{1_t \rightarrow 3_t}$ tautomerization processes exhibit smaller free energy barriers than the $\mathbf{1_o \rightarrow 3_o}$ transformation (by 7.56 and 7.48 kcal mol^{-1} for gas phase and ethanol solution, respectively). For assisted mechanisms the difference is less than half of the value predicted for the intramolecular mechanism. This is consistent with the results of Castro's experimental studies of reaction mechanisms and kinetics of thioketones.[29] It has been shown that thio–enethiol tautomerization is greatly favored relative to the enolization of carbonyl compounds. The calculated relative (to the $\mathbf{1_t}$ thio form) energy of the $\mathbf{3_t}$ enethiol form (16.61 kcal mol^{-1}) and the free energy barrier for $\mathbf{1_t \rightarrow 3_t}$ tautomerization (52.83 kcal mol^{-1}) are not significantly different from those calculated at the MP2(full)/6-31G* level for thioacetamide[26] (17.20 kcal mol^{-1} and 56.66 kcal mol^{-1}). The values of the free energies of the $\mathbf{1_t \rightarrow 4_t}$ and $\mathbf{1_o \rightarrow 4_o}$ tautomerizations are comparable, whereas in the assisted mechanisms the free energy barriers for 4-methyl-1,3-dihydro-2*H*-1,5-benzodiazepine-2-thione tautomerizations are smaller than those for 4-methyl-1,3-dihydro-2*H*-1,5-benzodiazepin-2-one.

A similar trend is found in the changes in the relative energies of tautomers and activation energies of tautomeric transformations in solution compared to energies in the gas phase for 4-methyl-1,3-dihydro-2*H*-1,5-benzodiazepin-2-one and 4-methyl-1,3-dihydro-2*H*-1,5-benzodiazepine-2-thione. For the diethanol- and self-assisted mechanisms the relative stability orders of the tautomers are similar for both series. When long-range solvent effects are taken into account the isolated $\mathbf{4_t}$ tautomer is found to be the most stable tautomer, lying 1.79 kcal mol^{-1} lower in energy than the $\mathbf{1_t}$ tautomer, whereas the relative energy of the $\mathbf{4_o}$ tautomer is evaluated as 0.14 kcal mol^{-1}. The activation barrier for the proton transfer from C(3) to N(5) in ethanol solution is therefore reversed in the case of 4-methyl-1,3-dihydro-2*H*-1,5-benzodiazepine-2-thione relative to that of 4-methyl-1,3-dihydro-2*H*-1,5-benzodiazepin-2-one and the relative stability order becomes as follows: $\mathbf{4_t > 1_t > 2_t > 3_t}$. A similar trend is also observed in the monosolvation case.

Population of Tautomers

The equilibrium constants for tautomerizations of 4-methyl-1,3-dihydro-2*H*-1,5-benzodiazepin-2-one and 4-methyl-1,3-dihydro-2*H*-1,5-benzodiazepine-2-thione were calculated by use of the standard formula $K = e^{-\Delta G/RT}$, the calculations being performed at T = 298.15 K. As can be seen in Table 9, the two keto forms are characterized by an equilibrium constant equal to 2.77×10^{-3}. Mono- and disolvation decrease the equilibrium constant slightly, to 2.08×10^{-3}, and 1.56×10^{-3}, respectively, shifting the equilibrium towards the $\mathbf{1_o \cdot et}$ and $\mathbf{1_o \cdot et_2}$ keto forms. Optimiza-

Table 9. Estimated equilibrium constants for intramolecular and ethanol-assisted tautomerizations of 4-methyl-1,3-dihydro-2*H*-1,5-benzodiazepin-2-one and 4-methyl-1,3-dihydro-2*H*-1,5-benzodiazepine-2-thione [B3LYP/6-311++G(d,p) and PCM/B3LYP/6-311++G(d,p) levels] and for diethanol-assisted tautomerizations [B3LYP/6-311++G(d,p)//B3LYP/6-31G(d) and PCM/B3LYP/6-311++G(d,p)//B3LYP/6-31G(d) levels].

Equilibrium	K_{eq} gas	ethanol solution	Equilibrium	K_{eq} gas	ethanol solution
$\mathbf{1_o \rightarrow 4_o}$	2.77×10^{-3}	0.79	$\mathbf{1_t \rightarrow 4_t}$	2.65×10^{-2}	20.51
$\mathbf{1_o \rightarrow 2_o}$	3.20×10^{-9}	1.01×10^{-9}	$\mathbf{1_t \rightarrow 2_t}$	8.38×10^{-7}	1.17×10^{-8}
$\mathbf{1_o \rightarrow 3_o}$	4.36×10^{-17}	3.20×10^{-14}	$\mathbf{1_t \rightarrow 3_t}$	6.68×10^{-13}	2.67×10^{-12}
$\mathbf{1_o \cdot et^c \rightarrow 4_o \cdot et}$	2.08×10^{-3}	24.18	$\mathbf{1_t \cdot et^c \rightarrow 4_t \cdot et}$	3.94×10^{-3}	45.35
$\mathbf{1_o \cdot et^a \rightarrow 2_o \cdot et}$	1.67×10^{-8}	2.52×10^{-9}	$\mathbf{1_t \cdot et^a \rightarrow 2_t \cdot et}$	2.38×10^{-8}	6.95×10^{-9}
$\mathbf{1_o \cdot et^b \rightarrow 3_o \cdot et}$	1.13×10^{-15}	3.02×10^{-13}	$\mathbf{1_t \cdot et^b \rightarrow 3_t \cdot et}$	8.38×10^{-14}	2.56×10^{-11}
$\mathbf{1_o \cdot et_2^c \rightarrow 4_o \cdot et_2}$	1.56×10^{-3}	6.06×10^{-4}	$\mathbf{1_t \cdot et_2^c \rightarrow 4_t \cdot et_2}$	7.19×10^{-2}	8.65×10^{-2}
$\mathbf{1_o \cdot et_2^a \rightarrow 2_o \cdot et_2}$	4.48×10^{-9}	1.50×10^{-9}	$\mathbf{1_t \cdot et_2^a \rightarrow 2_t \cdot et_2}$	5.91×10^{-10}	1.34×10^{-10}
$\mathbf{1_o \cdot et_2^b \rightarrow 3_o \cdot et_2}$	2.66×10^{-14}	8.30×10^{-15}	$\mathbf{1_t \cdot et_2^b \rightarrow 3_t \cdot et_2}$	3.04×10^{-14}	8.94×10^{-16}

tion of the tautomers by use of the PCM model reduces the gas-phase difference in energy between the pairs of isolated and monosolvated keto tautomers, leading to equilibrium constants of 0.79 and 24.18, respectively, and shifting the equilibrium towards the $\mathbf{4_o}$ and $\mathbf{4_o \cdot et}$ keto forms. Because the populations of the pairs of keto tautomers are similar, it might be expected that they should coexist in the gas phase and in ethanol solution. Experimental results suggest the presence of two keto forms of some substituted dihydro-1,5-benzodiazepin-2-ones.[8] In contrast, instability of enol forms in relation to keto forms and as the result their negligible populations explain the absence of enol tautomers in experimental studies.[7–12]

The equilibrium constants for 4-methyl-1,3-dihydro-2*H*-1,5-benzodiazepine-2-thione are larger than those for 4-methyl-1,3-dihydro-2*H*-1,5-benzodiazepin-2-one, whereas the trends of their changes in both series are similar.

The experimentally determined presence of one or two (thio)keto forms for substituted dihydro-1,5-benzodiazepin-2-ones[8] or dihydro-1,5-benzodiazepine-2-thiones[11] indicates that the imine–enamine tautomerization rate constant may be a more limiting factor than the equilibrium constant. The factors that might stabilize transition states of this type of tautomerization would promote the presence of both (thio)keto forms.

Conclusions

This work presents the first systematic quantum chemical investigation of the tautomeric equilibrium and proton-transfer mechanism of lactim–lactam, keto–enol, and imine–enamine tautomerizations in the isolated, monoethanol- and diethanol-solvated, and dimeric forms of 4-methyl-1,3-dihydro-2*H*-1,5-benzodiazepin-2-one and 4-methyl-1,3-dihydro-2*H*-1,5-benzodiazepine-2-thione, in the gas phase and in solution at the B3LYP/6-31G(d) and B3LYP/6-311++G(d,p) levels of theory. The study has clarified the tautomeric properties of these compounds in the gas phase and in two types of solutions (i.e., in protic and aprotic solvents).

The main conclusions are as follows:

1. The results of the calculations indicate that in the gas phase the keto forms are more stable than the enol tautomers. The order of stability for the tautomers of 4-methyl-1,3-dihydro-2*H*-1,5-benzodiazepin-2-one is as follows: $\mathbf{1_o > 4_o > 2_o > 3_o}$. Substitution of oxygen by sulfur diminishes the energy differences between the isolated tautomeric forms but the order of their stability is maintained. Similar relative stability orders were found for monoethanol- and diethanol-solvated tautomeric forms and for dimers of 4-methyl-1,3-dihydro-2*H*-1,5-benzodiazepin-2-one and 4-methyl-1,3-dihydro-2*H*-1,5-benzodiazepine-2-thione in the gas phase. The gas-phase relative free energies and equilibrium constants for the tautomers of both series vary in solution relative to the gas phase, resulting in shifts of the equilibria upon solvation. Because of its larger dipole moment, the N(5)–H keto (thio) tautomer may be preferentially stabilized in ethanol environments and in other polar solvents. Therefore, when solvent effects are taken into account, the relative stability orders of the two thio forms reverse, relative to the gas-phase equilibria, in the cases of the isolated and the monoethanol-solvated forms of 4-methyl-1,3-dihydro-2*H*-1,5-benzodiazepine-2-thione. The obtained results predict detectable populations of both (thio)keto tautomers in both series both in the gas phase and in solution. This is consistent with experimental results suggesting the presence of two (thio)keto forms of some substituted dihydro-1,5-benzodiazepin-2-ones and dihydro-1,5-benzodiazepine-2-thiones.[8,11]

2. The intramolecular proton-transfer reactions for all studied tautomerization processes are characterized by very high free energy barriers, and so do not take place in the ground state. Explicit inclusion of an ethanol molecule in the proton-transfer reaction path reduces the barrier height drastically, making the process possible. The effect on the kinetics of lactim–lactam tautomerization of a second ethanol molecule in the bridging site is not significant, but disolvation substantially reduces the free energy barriers for imine–enamine and keto(thio)–enol(enethiol) tautomerizations, so the participation of two ethanol molecules in a proton transfer reaction should be considered for better description of the tautomeric properties of 4-methyl-1,3-dihydro-2*H*-1,5-benzodiazepin-2-one and 4-methyl-1,3-dihydro-2*H*-1,5-benzodiazepine-2-thione in ethanol solution. We found that the free energy barriers of the self-assisted mechanism are about half the height of those for uncata-

lyzed intramolecular proton transfer. For 4-methyl-1,3-dihydro-2*H*-1,5-benzodiazepin-2-one the decreases in the free energy barriers in self-assisted mechanisms relative to intramolecular process are larger than those for 4-methyl-1,3-dihydro-2*H*-1,5-benzodiazepine-2-thione for the lactim–lactam and keto–enol tautomerizations, but for imine–enamine tautomerization they are smaller.

We believe that the potential tautomeric transformations of 2,3-dihydro-1,5-benzodiazepin-2-ones and their thio analogues reported in this paper should be useful for investigation of interaction mechanisms of these compounds with various chemical reagents and cell receptors.

Supporting Information (see also the footnote on the first page of this article): Total energies and Gibbs free energies tabulated for all related compounds and imaginary frequencies for all transition states (Table S1–S4), optimized geometrical parameters of tautomers and transition states for direct and ethanol-assisted tautomerizations at the B3LYP/6-311++G(d,p) and PCM/B3LYP/6-311++G(d,p) levels (Table S5–S10), optimized geometrical parameters of tautomers and transition states for diethanol- and self-assisted tautomerizations at the B3LYP/6-31G(d) level (Tables S11–S14), and evaluation of bond lengths and energy changes by IRC calculations for the catalytic tautomerization of the 4-methyl-1,3-dihydro-2*H*-1,5-benzodiazepin-2-one (Figures S1–S10).

Acknowledgments

This work has been supported by the National Science Foundation (NSF CREST) HRD-0833178. The computation time was provided by the Mississippi Centre for Supercomputer Research.

[1] a) R. Janciene, Z. Stumbreviciute, A. Vektariene, L. Kosychova, R. Sirutkaitis, A. Palaima, Z. Staniulyte, B. D. Puodziunaite, *Heteroat. Chem.* **2008**, *19*, 72–81; b) D. Nardi, A. Tajana, S. Rossi, *J. Heterocycl. Chem.* **2009**, *10*, 815–819; c) R. Janciene, Z. Stumbreviciute, D. Podeniene, B. D. Puodziunaite, S. Black, S. M. Husbands, *J. Heterocycl. Chem.* **2006**, *43*, 979–984; d) F. Ayala-Guerrero, C. Blanco, U. Guevara, J. Taboada, R. Martinez, A. Campos, *Proc. West Pharmacol. Soc.* **1992**, *35*, 153–155; e) R. Gharbi, M. Ben-Youssef, M.-T. Martin, Z. Mighri, *J. Chem. Res., Synop.* **2005**, *4*, 257–261; f) S. El Hazazi, A. Baouid, A. Hasnaoui, M. Pierrot, *Acta Crystallogr., Sect. C* **2002**, *58*, 585–588; g) R. Janciene, L. Kosychova, V. Bukelskiene, V. Domkus, Z. Stumbreviciute, V. Ragaleviciene, B. D. Puodziunaite, *Arzneim.-Forsch.* **2002**, *52*, 475–481.

[2] a) W. Nawrocka, B. Sztuba, M. Rutkowska, J. Barczyńska, A. Opolski, J. Wietrzyk, *Acta Pol. Pharm.* **1998**, *55*, 397–402; b) W. Nawrocka, H. Liszkiewicz, A. Nawojski, M. Wilimowski, L. Kedzierska-Goździk, J. Barczyńska, W. Wojewódzki, E. Duś, A. Szelag, M. Rutkowska, *Pol. J. Pharmacol. Pharm.* **1991**, *43*, 495–503; c) F. Savelli, A. Boido, A. Mulè, L. Piu, M. C. Alamanni, G. Pirisino, M. Satta, A. Peana, *Farmaco* **1989**, *44*, 125–140.

[3] a) Z. F. Solomko, V. N. Proshkina, N. Ya. Boganova, USSR Inventor's Certificate # 1072433, **1982**; b) N. Ya. Boganova, V. N. Proshkina, Z. F. Solomko, USSR Inventor's Certificate # 1198917, **1984**; c) Z. F. Solomko, V. N. Proshkina, M. P. Hmel, USSR Inventor's Certificate # 1295700, **1985**; d) Z. F. Solomko, E. T. Zlenko, A. A. Gaponov, E. M. Demchenko, USSR Inventor's Certificate # 1586135, **1988**; e) Z. F. Solomko, E. T. Zlenko, A. A. Gaponov, USSR Inventor's Certificate # 1633779, **1989**; f) A. Bauer, P. Danneberg, K.-H. Weber, K. Minck, *J. Med. Chem.* **1973**, *16*, 1011–1014; g) R. C. Haris, J. M. Straley, U. S. Patent 1 537 757, **1968**, *Chem. Abstr.* **1970**, *73*, 100054w; h) J. R. De Baun, F. M. Pallos, D. R. Baker, U. S. Patent 3 978 227, **1976**, *Chem. Abstr.* **1977**, *86*, 5498d.

[4] D. A. Horton, G. T. Bourne, M. L. Smythe, *Chem. Rev.* **2003**, *103*, 893–930.

[5] a) E. M. Essassi, M. Salem, *Bull. Soc. Chim. Belg.* **1988**, *97*, 387–394; b) J. N. T. Ghomsi, N. H. Ahabchane, E. M. Essassi, *Phosphorus Sulfur Silicon Relat. Elem.* **2004**, *179*, 353–364; c) M. L. Doumbia, R. Bouhfid, N. H. Ahabchane, E. M. Essassi, *ARKIVOC* **2008**, *13*, 36–44.

[6] a) A. Akdag, M. L. McKee, S. D. Worley, *J. Phys. Chem. A* **2006**, *110*, 7621–7627; b) F. H. Westheimer, *Proc. Chem. Soc. London* **1963**, 253–261; c) W. Tagaki, F. H. Westheimer, *Biochemistry* **1968**, *7*, 901–905; d) R. D. Kobes, E. E. Dekker, *Biochem. Biophys. Res. Commun.* **1967**, *27*, 607–612.

[7] R. Benassi, P. Lazzeretti, F. Taddei, D. Nardi, A. Tajana, *Org. Magn. Reson.* **1976**, *8*, 387–388.

[8] Y. Kurasawa, Y. Okamoto, K. Ogura, A. Takada, *J. Heterocycl. Chem.* **1985**, *22*, 661–664.

[9] E. C. Cortes, M. M. Torres, *J. Heterocycl. Chem.* **1997**, *34*, 953–956.

[10] E. C. Cortes, C. M. A. Castrejon, *J. Heterocycl. Chem.* **1997**, *34*, 1809–1812.

[11] a) D. Nardi, A. Tajana, S. Rossi, *J. Heterocycl. Chem.* **1973**, *10*, 815–819; b) A. A. Stoliarchyk, I. N. Phyrman, V. L. Pikalov, Z. P. Solomko, V. S. Tkachenko, *Chem. Pharm. J.* **1975**, *9*, 19–21; c) Z. P. Solomko, P. A. Sharbatyan, A. A. Gaponov, V. I. Avramenko, *Chem. Heterocycl. Compd.* **1990**, *3*, 396–400.

[12] a) B. A. Puodzhyunaite, Z. A. Talaikite, *Chem. Heterocycl. Compd.* **1974**, *6*, 833–837; b) T. S. Chmilenko, Z. Ph. Solomko, A. N. Kost, *Chem. Heterocycl. Compd.* **1977**, *13*, 423–427.

[13] J. Elguero, C. Marzin, A. R. Katritzky, P. Linda, *The Tautomerism of Heterocycles* in *Advances in Heterocyclic Chemistry* (Eds.: A. R. Katritzky, A. J. Boulton), Academic Press, New York, **1976**, suppl. 1, pp. 560–564.

[14] a) C.-H. Chuang, M.-H. Lien, *J. Phys. Chem. A* **2004**, *108*, 1790–1798; b) P. Li, Y. Bu, *J. Phys. Chem. A* **2004**, *108*, 10288–10295; c) P. I. Nagy, F. R. Tejada, W. S. Messer, *J. Phys. Chem. B* **2005**, *109*, 22588–22602; d) A. M. Lamsabhi, *J. Phys. Chem. A* **2008**, *112*, 1791–1797.

[15] a) A. Fu, H. Li, D. Du, Z. Zhou, *J. Phys. Chem. A* **2005**, *109*, 1468–1477; b) A. M. El-Nahas, M. J. Mphahlele, *THEOCHEM* **2004**, *668*, 157–162; c) A. Contini, D. Nava, P. Trimarco, *J. Org. Chem.* **2006**, *71*, 159–166.

[16] a) E. M. Essassi, J.-P. Lavergne, P. Viallefont, *Tetrahedron* **1977**, *33*, 2807–2812; b) E. M. Essassi, M. Salem, *Bull. Soc. Chim. Belg.* **1985**, *94*, 755–758.

[17] a) E. S. Kryachko, M. T. Nguyen, T. Zeegers-Huyskens, *J. Phys. Chem. A* **2001**, *105*, 1288–1295; b) Q.-S. Li, W.-H. Fang, J.-G. Yu, *J. Phys. Chem. A* **2005**, *109*, 3983–3990; c) M. K. Shukla, J. Leszczynski, *J. Phys. Chem. A* **2005**, *109*, 7775–7780; d) V. Enchev, N. Markova, S. Angelova, *J. Phys. Chem. A* **2005**, *109*, 8904–8913; e) H.-S. Kim, D.-S. Ahn, S.-Y. Chung, S. K. Kim, S. Lee, *J. Phys. Chem. A* **2007**, *111*, 8007–8012.

[18] Z. Yang, M. T. Rodgers, *Phys. Chem. Chem. Phys.* **2004**, *6*, 2749–2757.

[19] M. K. Shukla, J. Leszczynski, *J. Phys. Chem. A* **2000**, *104*, 3021–3027.

[20] a) A. D. Becke, *J. Chem. Phys.* **1993**, *98*, 5648–5652; b) A. D. Becke, *J. Chem. Phys.* **1993**, *98*, 1372–1377; c) C. Lee, W. Yang, R. G. Parr, *Phys. Rev. B* **1988**, *37*, 785–789.

[21] a) S. Mierts, E. Scrocco, J. Tomasi, *Chem. Phys.* **1981**, *55*, 117–129; b) M. Cossi, B. Mennucci, J. Tomasi, *Chem. Phys. Lett.* **1994**, *228*, 165–170.

[22] C. Gonzales, H. B. Schlegel, *J. Phys. Chem.* **1989**, *90*, 2154–2161.

[23] A. P. Scott, L. Radom, *J. Phys. Chem.* **1996**, *100*, 16502–16513.

[24] M. J. Frisch, G. W. Trucks, H. B. Schlegel, G. E. Scuseria, M. A. Robb, J. R. Cheeseman, J. A. Montgomery Jr., T. Vreven, K. N. Kudin, J. C. Burant, J. M. Millam, S. S. Iyengar, J. Tomasi, V. Barone, B. Mennucci, M. Cossi, G. Scalmani, N.

Rega, G. A. Petersson, H. Nakatsuji, M. Hada, M. Ehara, K. Toyota, R. Fukuda, J. Hasegawa, M. Ishida, T. Nakajima, Y. Honda, O. Kitao, H. Nakai, M. Klene, X. Li, J. E. Knox, H. P. Hratchian, J. B. Cross, V. Bakken, C. Adamo, J. Jaramillo, R. Gomperts, R. E. Stratmann, O. Yazyev, A. J. Austin, R. Cammi, C. Pomelli, J. W. Ochterski, P. Y. Ayala, K. Morokuma, G. A. Voth, P. Salvador, J. J. Dannenberg, V. G. Zakrzewski, S. Dapprich, A. D. Daniels, M. C. Strain, O. Farkas, D. K. Malick, A. D. Rabuck, K. Raghavachari, J. B. Foresman, J. V. Ortiz, Q. Cui, A. G. Baboul, S. Clifford, J. Cioslowski, B. B. Stefanov, G. Liu, A. Liashenko, P. Piskorz, I. Komaromi, R. L. Martin, D. J. Fox, T. Keith, M. A. Al-Laham, C. Y. Peng, A. Nanayakkara, M. Challacombe, P. M. W. Gill, B. Johnson, W. Chen, M. W. Wong, C. Gonzalez, J. A. Pople, *Gaussian03*, revision B.05, Gaussian, Inc., Wallingford CT, **2004**.

[25] N. Markova, V. Enchev, I. Timtcheva, *J. Phys. Chem. A* **2005**, *109*, 1981–1988.

[26] C.-C. Su, C.-K. Lin, C.-C. Wu, M.-H. Lien, *J. Phys. Chem. A* **1999**, *103*, 3289–3293.

[27] E. P. Z. Wigner, *Z. Phys. Chem. Abt. B* **1932**, *19*, 203–216.

[28] a) A. Nallini, K. Saraboji, M. N. Ponnuswamy, M. Verkatrai, R. Jeyaraman, *Cryst. Res. Technol.* **2005**, *40*, 622–626; b) A. B. Bogatskij, S. A. Andronati, N. I. Golovenko, *Tranquilizators* (Eds.: V. P. Kukhar), Kyiv, **1980**, pp. 85–100.

[29] E. A. Castro, *Chem. Rev.* **1999**, *99*, 3505–3524.

Received: June 21, 2009
Published Online: November 18, 2009

